

# Eco-Friendly Synthesis of Copper Nanoparticles: Characterization Using Bioflocculant from *Microbacterium paraoxydans*

Nokwanda P. Myeni<sup>1</sup>, Albertus K. Basson<sup>1</sup>, Zuzingcebo G. Ntombela<sup>1</sup>,  
Rajasekhar V.S.R. Pullabhotla<sup>2,\*</sup> 

<sup>1</sup> Department of Biochemistry and Microbiology, Faculty of Science, Agriculture and Engineering, University of Zululand, P/Bag X001, KwaDlangezwa 3886, South Africa

<sup>2</sup> Department of Chemistry, Faculty of Science, Agriculture, and Engineering, University of Zululand, P/Bag X001, KwaDlangezwa 3886, South Africa

\* Correspondence: PullabhotlaV@unizulu.ac.za;

Received: 29.09.2024; Accepted: 11.04.2025; Published: 7.09.2025

**Abstract:** The production of microbial-based nanoparticles has various advantages over conventional physicochemical procedures and has many applications in medicine and biology. In this study, bioflocculant extracted from *Microbacterium paraoxydans* was applied to biosynthesize CuNPs. The biosynthesized CuNPs and the bioflocculant were analyzed using UV-Vis, FT-IR, SEM-EDX, TGA, XRD, and TEM. The UV-visible spectra of CuNPs presented a peak at 549 nm, corresponding to the plasmon absorbance of CuNPs. TEM image revealed spherical CuNPs with an average size ranging between 30-35 nm, indicating a role of the bioflocculant as a capping and reducing agent in CuNP synthesis. The XRD analysis for CuNPs showed the crystalline nature and CuNPs with a 33 nm particle size. FT-IR analysis of CuNPs discovered the presence of various functional groups, including the O-H bond, C-H, N-H, and Cu-O bond. SEM showed the cloud-like surface morphology of CuNPs, while the bioflocculant indicated surface rod-shaped morphology. The elemental analysis of CuNPs revealed the presence of oxygen, carbon, and copper, and the bioflocculant has carbon and oxygen. The CuNPs appeared to be thermostable as they retained a weight of 75% at 900°C. The characterization confirmed the successful synthesis of CuNPs utilizing a bioflocculant as a stabilizing and capping agent.

**Keywords:** biosynthesis; *Microbacterium paraoxydans*; bioflocculant; copper nanoparticles and characterization.

© 2025 by the authors. This article is an open-access article distributed under the terms and conditions of the Creative Commons Attribution (CC BY) license (<https://creativecommons.org/licenses/by/4.0/>), which permits unrestricted use, distribution, and reproduction in any medium, provided the original work is properly cited. The authors retain copyright of their work, and no permission is required from the authors or the publisher to reuse or distribute this article, as long as proper attribution is given to the original source.

## 1. Introduction

Flocculation is a physical procedure whereby flocculants are applied in the agglomeration of suspended particles to produce large flocs, which are masses of solids that can be organic or inorganic [1,2]. Flocculants are categorized into three kinds: organic synthetic, inorganic chemical, and natural flocculants. Organic synthetic flocculants include polyacrylic and polyaluminium, inorganic chemical flocculants include polyacrylamide derivatives and aluminum sulfate, and naturally occurring flocculants include microbial flocculants, tannin, and chitosan [3]. Industries and wastewater treatment facilities commonly use both synthetic organic and inorganic chemical flocculants due to their competence and cost-effectiveness [4]. However, synthetic flocculants constitute a risk to the environment and

human health [5]. These drawbacks associated with synthetic flocculants have led to the synthesis of eco-friendly, strong, economically feasible, and biodegradable flocculants for wastewater treatment. Bioflocculants have been identified as a promising substitute for chemical flocculants in the future [4, 6].

Bioflocculants are described as polymers extracted from microbes during their growth, which floc out suspended particles in a solution [7,8]. Bioflocculants have benefits such as a lack of secondary pollution and biodegradability, and they are nontoxic; hence, they are suitable for the replacement of chemical flocculants [9]. Bioflocculation refers to a treatment procedure in which bioflocculants are utilized in the agglomeration of suspended particles [3]. Bioflocculation is well-thought-out as a dynamic process initiated by living cells as a result of the production of exopolymeric macromolecules [10]. Bioflocculants have shortcomings such as low flocculation efficiency, low yield, high cost, and shorter shelf-life, and they are unable to floc out microbial pollutants [11]. Hence, there is a growing interest in the biosynthesis of copper nanoparticles to enhance their yield and flocculating efficiency.

Nanotechnology is a science and technology that focuses on creating and understanding materials that range between 1 to 100 nm [12]. Copper nanoparticles gained tremendous interest due to their exceptional properties, including electrical conductivity, high melting point, reduced electrochemical migration risk, economical, and excellent solder ability [13, 14]. For this reason, copper nanoparticles serve as a favorable candidate to replace high-cost noble metal nanoparticles such as Ag and Au [15]. Copper nanoparticles also possess unique physicochemical properties such as catalytic, antimicrobial activity, low production cost, and efficiency [16]. The production of copper nanoparticles can occur through either a physical or a chemical process [17]. The chemical method includes chemical reduction and thermal decomposition. The physical method includes laser ablation and mechanical chemical synthesis [18].

Metallic copper nanoparticles are unstable, meaning they can be oxidized under atmospheric environments, forming  $\text{Cu}_2\text{O}$  and/ or  $\text{CuO}$  on the surface throughout the preparation [19]. Thus, copper nanoparticles should be protected by the addition of stabilizing agents such as organic ligands, surface-active agents, or capping agents that can form complexes with copper ions [15]. Copper nanoparticles exhibit a small size with a very strong catalytic surface area with substantial permeability. These nanoparticles can achieve increased reaction yields in a quicker reaction period when exploited as chemical reactants in organic and inorganic metallic production [20, 21]. Therefore, the study focused on the biosynthesis and characterization of copper nanoparticles by utilizing a bioflocculant as a stabilizing and reducing agent. Bioflocculant was exploited in the biosynthesis of copper nanoparticles to enhance the yield and flocculating efficiency. The biosynthesized CuNPs were characterized to confirm their successful synthesis employing UV-vis spectroscopy, SEM-EDX, FT-IR, TEM, TGA, and XRD.

## 2. Materials and Methods

### 2.1. Bioflocculant extraction and purification.

To extract and purify the bioflocculant, the technique defined by Ntombela et al. [22] was used. After an optimal fermentation period, the fermented production suspension was centrifugated at 4000 rpm for 30 min to eliminate cell debris. The insoluble materials were eliminated by adding 1 L of distilled water to the upper solution and centrifuged at 4000 rpm

for 30 min. The supernatant obtained after centrifugation was mixed with 2 L of ice-cold ethanol. The mixture was stirred thoroughly and precipitated at 4°C for 12 h. The sediment was removed and vacuum-dried to attain a crude bioflocculant extract. The crude bioflocculant extract was purified by redissolving it in 100 mL of a dissolution of chloroform and butanol (5:2 w/v) and stirring to mix. Subsequently, the dissolution was then permitted to sit for 12 h at room temperature. The purified bioflocculant was removed aseptically and air-dried.

### 2.2. Biological production of copper nanoparticles.

The bio-reduction method using the bioflocculant from *Microbacterium paraoxydans* was employed in synthesizing copper nanoparticles. About 0.5 g of the pure bioflocculant was dissolved into a 200 mL dissolution of 3 Mm CuSO<sub>4</sub>. The solution was vigorously shaken to attain a homogeneous solution. The interference of foreign materials was prevented by sheeting the conical flask, holding the solution with the foil, and leaving it undisturbed at ambient room temperature for a period of 24 hours. The mixture without the addition of bioflocculant was used as a standard in this experiment. Characterization and physical observation were used to confirm the synthesis of CuNPs. After 24 h, the biosynthesized CuNPs were gathered using centrifugation at 4°C, 400 rpm for 30 min. The biosynthesized CuNPs were then air-dried for 72 h and stored for characterization and application.

### 2.3. Characterisation of a purified bioflocculant and biosynthesized copper nanoparticles.

The ability of the bioflocculant and CuNPs to absorb light was measured using the UV-vis of the Perkin-Elmer spectrophotometer (Agilent Technologies, California 95051, USA). About 0.1 g of the bioflocculant and CuNPs samples were diluted with 3 mL of deionized water. The analysis was carried out within the wavelength of 300 -700 nm, operating at 1 nm resolution [23].

The functional group identification of the bioflocculant and bioflocculant-encapsulated CuNPs was accomplished using FT-IR (Perkin Elmer System 2000, Cambridge, England). A small amount of the produced copper nanoparticles and purified bioflocculant was pressed into a pellet for FT-IR spectroscopy analysis over a range of 4000 - 400 cm<sup>-1</sup> wavelength [24].

TEM was conducted to ascertain the particle size and morphology of the bioflocculant and copper nanoparticles. TEM (JOEL 1010 USA, Inc, Peabody, Massachusetts 01960, USA) was probed to acquire the TEM depiction of a bioflocculant and copper nanoparticles. The beam of light was passed through a sample to generate an image. The samples were prepared, and the micropipette was used to add a diluted drop of suspension in a solvent. The samples were allowed to dry at ambient room temperature. The 100 kV accelerating voltage was used to observe the samples, and the results were taken using a digital camera [25].

TGA analysis of the bioflocculant and the synthesized CuNPs was performed to study the change in mass of a substance while the temperature of the substance changes over time. The thermogravimetric analyzer (ST6A 449/C Jupiter, Netsch, Wittlsbacherstrabe, Germany) was adjusted to the temperature ranges of 30 - 900°C under a continual flow of nitrogen gas [26].

SEM analysis of the bioflocculant and the produced CuNPs was done to determine their morphology. The produced Cu nanoparticles and bioflocculant images were obtained and viewed using an SEM-primed elementary detector at 15 kV, which was a wavelength of resolution. The produced CuNPs and purified bioflocculant were analyzed for their

morphology. SEM-EDX (Hitachi SU230 Regulus FESEM at Surface Science Western, Cape) was used to identify the elemental arrangement of copper nanoparticles and biofloculant. Copper nanoparticles and the biofloculant. Scanning electron microscopy equipped with energy-dispersive X-ray spectroscopy was used to determine the elements present in both the biofloculant and copper nanoparticles [27].

XRD (Bruker D8 Advance diffractometer, Johannesburg, Bruker, RSA) was used to analyze the crystalline nature of the samples. X-ray was used to irradiate the copper nanoparticles and biofloculant samples, and then intensity and scattering angles were measured. The angle range of 20 to 80° was used at the scanning step of 0.03° was used to record the XRD results [28]. The average particle size of CuNPs biosynthesized from *M. paraoxydans* biofloculant was determined employing Debye-Scherrer's equation [ $D = (k\lambda / \beta \cos \theta)$ ] where D is the size of the particle, K (0.94) is the Scherrer's constant,  $\lambda$  (1.54178Å) is the wavelength, and  $\beta$  is the width at half maximum of the diffraction peak [29].

### 3. Results and Discussion

#### 3.1. Biofloculant extraction and purification.

The biofloculant was extracted and purified using different solvents, including ethanol, chloroform, and butanol. The biofloculant of about 3.5 g was acquired from 1000 mL of culture broth after purification. The obtained yield is much improved when equated to the yield produced previously. For example, Ntombela et al. [30] reported a 1.5 g/L yield manufactured from *Bacillus sp.*, and Makapela et al. [31] produced a 2.5 g biofloculant yield from *Bacillus pumilus*. On the other hand, *Microbacterium esteraromaticum* C26 produced a cation-dependent biofloculant with a high yield of 4.92 g/L under optimized conditions [32]. Nevertheless, *M. paraoxydans* has the potential to produce a biofloculant with a high yield. More optimization of the biofloculant production conditions could improve the yield.

#### 3.2. Biological synthesis of copper nanoparticles.

Copper nanoparticles were successfully biosynthesized from the biofloculant and CuSO<sub>4</sub>. The successful synthesis of copper nanoparticles was observed through a change in color from colorless to blueish. The bluish color is possibly linked to surface plasmon resonance. Other authors also reported the change in color from colorless to blueish, confirming the synthesis of CuNPs using biofloculant as a capping and reducing agent. Dlamini et al. [17] also described the production of CuNPs utilizing a biofloculant from *Alcaligenes faecalis* HCB2. The successful synthesis of CuNPs examining a biofloculant as a stabilizing and reducing agent was further confirmed through their characterization using UV-spectroscopy, FTIR, SEM-EDX, TEM, TGA, and XRD.

#### 3.3. Characterisation of a biofloculant and copper nanoparticles.

The biosynthesized copper nanoparticles and a pure biofloculant were evaluated for their characteristics using different analysis methods, including UV-spectroscopy, FTIR, SEM-EDX, TEM, TGA, and XRD analysis.

### 3.3.1. UV-visible spectroscopy analysis.

The bio-reduction of the aqueous copper ions and optical properties were determined using UV-visible spectroscopy [33]. The biofloculant UV-Vis spectrum (Figure 1) presented an absorption peak of nucleic acids at 260 nm, revealing that the biofloculant may be composed of nucleic acids. Dlamini et al. [34] reported an absorption peak between 290 – 300 nm for both the biofloculant and biosynthesized CuNPs. The absorption peak at 260 nm of the biofloculant is a characteristic associated with the presence of nucleic acids [35]. The UV-visible spectral analysis was used to determine different characteristics of CuNPs for the biological macromolecules present, and organic compounds and metal ions were determined using UV-Vis spectral analysis [36].

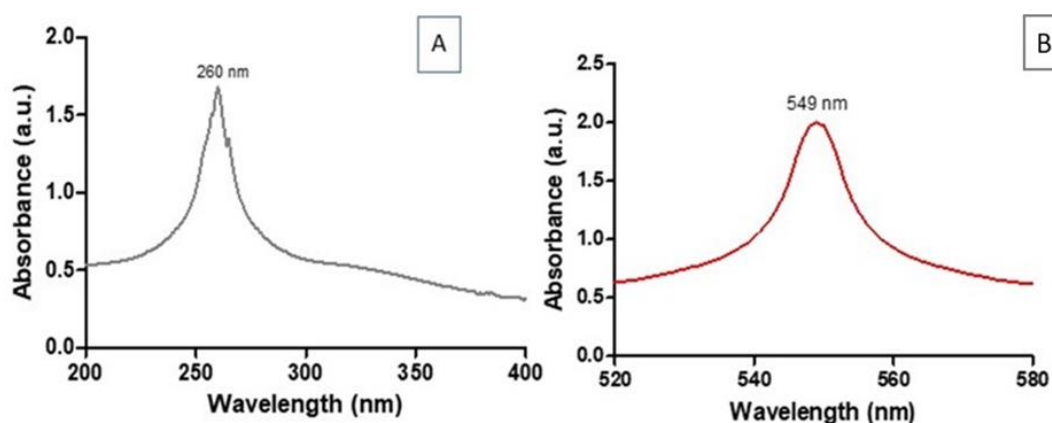


**Figure 1.** UV- visible analysis spectra of the (a) pure biofloculant; (b) CuNPs.

The color change from clear to blue was attributable to the characteristic surface plasmon resonance (SPR) shown by CuNPs. The biosynthesized CuNPs from a biofloculant extracted from *M. paraoxydans* exhibited an absorption peak around 549 nm due to its SPR absorption band (Figure 1b). The UV-Vis spectrum exhibited a single SPR band, revealing the shape of CuNPs, which was also confirmed by TEM. Amer and Awwad. [37] reported the CuNPs to exhibit a peak around 579 nm due to their SPR. An absorption peak at 550 nm was reported for the CuNPs synthesized from *Shewanella lothica* PV-4 (Gram-negative bacteria) [38]. The absorption peak at 551 nm was identified by the UV-Vis spectrum, which in the CuNPs biosynthesized by *Agaricus bisporus* [39]. CuNPs biosynthesized from *S. aromaticum* bud extracts revealed a peak at 580 nm in the UV-Vis spectrum [40].

### 3.3.2. FT-IR analysis of a biofloculant and biosynthesized CuNPs.

The biofloculant and biosynthesized CuNPs were characterized for their functional groups available in their molecular chain using FT-IR spectroscopy. The biofloculant FT-IR spectra showed significant peaks at 3424, 3303, 1818, 1055, 1023, 1028  $\text{cm}^{-1}$  (Figure 2). Different functional groups revealed are O-H, C-H, N-H, and C-O groups. A peak detected at 3424  $\text{cm}^{-1}$  was accredited to O-H stretching and is associated with moisture content. A peak observed at 1818  $\text{cm}^{-1}$  matched that of the C-H bond of indole functional groups. A peak observed at 1055  $\text{cm}^{-1}$  showed the C-O bond. A peak at 3303  $\text{cm}^{-1}$  is associated with N-H stretching, which confirms the polymerization of the flocculant. The hydroxyl group favored the presence of carbonyl groups, which signifies the thermostability of the biofloculant and solubility of the biofloculant in aqueous solution [41]. The carbonyl group present allows the

adsorption forces of the biofloculant particles to attach, while the hydroxyl group present in the biofloculant is formulated particularly for hydrophilic in the water environment [42]. The carbonyl and hydroxyl groups are used for the bridging mechanism and charge neutralization of the biofloculant [43]. The small stretching peak at  $2130\text{ cm}^{-1}$  in the biofloculant represents the isothiocyanate ( $\text{N}=\text{C}=\text{S}$ ) functional group. The absorption peak at  $554\text{ cm}^{-1}$  represented the presence of halo compounds, including carbon, chlorine, and bromide. The chemical composition of the biofloculant that is presented by their functional groups in the molecular chain length influences the flocculating activity of the pure biofloculant [44]. In the study by Xiong et al. [45], the biofloculant appeared to have hydroxyl, amine, and amide groups in its molecular chain. Similar observations were presented whereby the biofloculant was revealed to have functional groups such as O-H, N-H, C-O, and C-OH in its molecular chain [46].

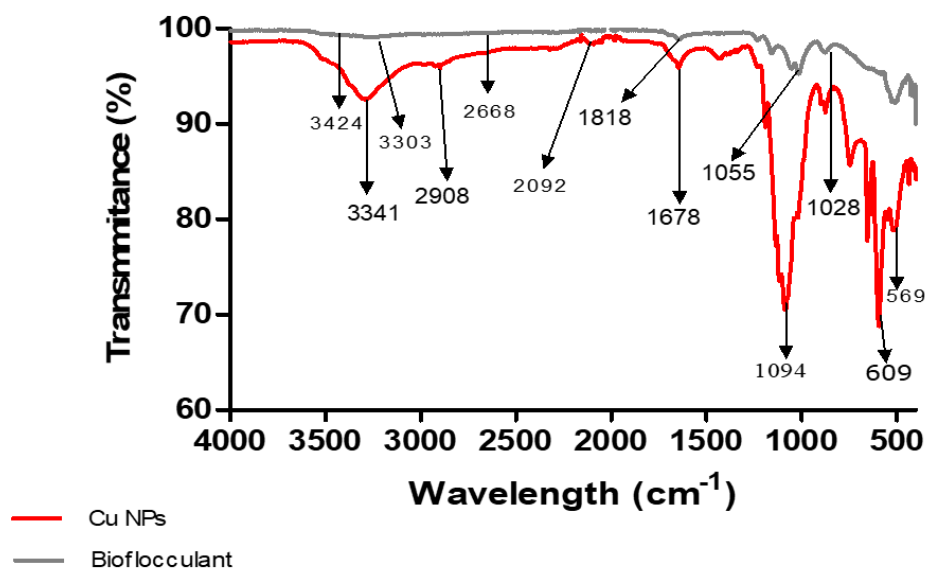


**Figure 2.** FT-IR spectra of the biofloculant and biosynthesized CuNPs.

The CuNPs biosynthesized from the biofloculant gain the ability to remove the pollutants from the functional groups found in their molecular structure. Therefore, the FT-IR analysis of CuNPs was studied, and the FT-IR spectrum was presented for different functional groups (Figure 2). The FT-IR spectrum showed the O-H stretching group from a compound class of intermolecular bonds in the peak of  $3341\text{ cm}^{-1}$ . The peak at  $2908\text{ cm}^{-1}$  revealed the N-H bond,  $2092\text{ cm}^{-1}$  revealed the presence of C-H, and  $569\text{ cm}^{-1}$  represented the presence of Cu-O. Functional groups present in CuNPs are liable for their flocculation efficiency. Mohamed [47] revealed the presence of  $3337.25$ ;  $2921.72$ ;  $1656.45$ ;  $1606.70$ ;  $1452.55$ ;  $1398.69$ ;  $1163.39$  and  $1097.44\text{ cm}^{-1}$ , which represented O-H stretching vibrations, C=C aromatic ring C-H asymmetric stretching, C=C, and C-OH stretching vibration stretching. The absorption peak shown by  $605.65\text{ cm}^{-1}$  characterized the Cu-O bond in CuNPs biosynthesized from *Syzygium Cumin* leaf extract [48].

### 3.3.3. SEM-EDX analysis of biofloculant and As-synthesized CuNPs.

The elemental composition of CuNPs and the biofloculant were analyzed using SEM-EDX. Elemental analysis of both the biofloculant and CuNP nanoparticles was conducted using SEM-EDX, and the results are displayed below (Figure 3).

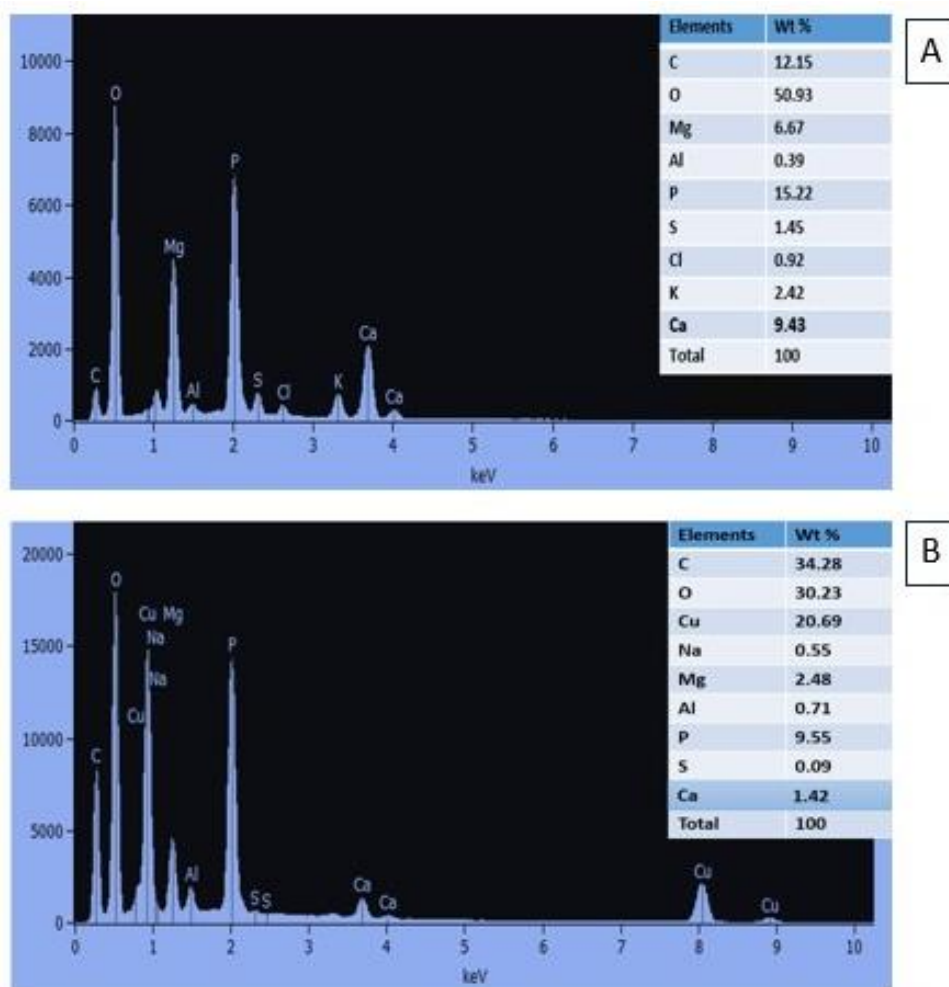


**Figure 3.** SEM-EDX analysis of a pure biofloculant and biosynthesized.

Elemental analysis from the SEM-EDX spectrum of the biofloculant revealed different elements, including C (12.15 wt %), O (50 wt %), Mg (6.67 wt %), Al (0.39 wt %), P (15.22 wt %), S (1.45 wt %) Cl (0.9 wt %), K (2.42 wt %), and Ca (9.43 wt %) (Figure 3a). The elements present can influence the flexibility and stability of the biofloculant [49]. Oxygen has the highest weight of 50.93 wt %, and C has a low weight of 12.15 wt %. The elements (C and O) present in the biofloculant confirm the polysaccharide nature of the biofloculant [50]. Ntombela et al. [46] investigated the elements of a purified biofloculant and reported the presence of C (50.22 wt %), O (38.07 wt %), Na (1.26 wt %), Mg (0.12 wt %), Al (0.11 wt %), P (0.86 wt %), S (3.06 wt %), Cl (0.97 wt %), K (2.11 wt %) and Ca (3.22 wt %).

Elemental analysis of the As-synthesized CuNPs was determined through the SEM-EDX spectrum. The elements in CuNPs can reveal their flexibility and stability [46]. Figure 3 illustrates the elements present in the molecular chain of CuNPs. The elemental composition of CuNPs showed the presence of Carbon (34.28 wt %), O (30.23 wt %), C (20.69 wt %), P (9.55 wt %), S (0.09 wt %), Ca (1.42 wt %), Na (0.55 wt %), Al (0.71 wt %) and Mg (2.48 wt %). The biosynthesized CuNPs were revealed to have a major content of carbon (34.28 wt %) and oxygen (30.23 wt %), confirming that they are synthesized from a polysaccharide biofloculant. Copper weighed 20.69 wt %; therefore, the CuNPs were confirmed to be successfully biosynthesized. El-Saadony et al. [51] also reported the elemental analysis of the biosynthesized CuNPs, and the elements displayed include Cu (13.21 wt %) and O (22.55 wt %).

### 3.3.4. SEM analysis of the biofloculant and biosynthesized CuNPs.

The scanning electron microscopy analysis was carried out to determine the surface morphological structure of the biofloculant and copper nanoparticles, and the images are displayed in Figure 4.

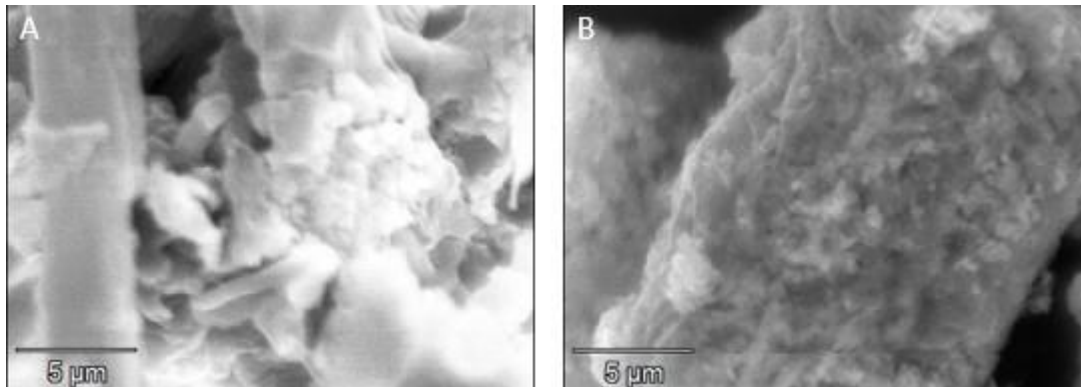


**Figure 4.** SEM images of a (a) purified biofloculant; (b) As-synthesized CuNPs at 100 nm.

A rod-shaped biofloculant is depicted in Figure 4a. The rod shape of the biofloculant proves that the biofloculant is crystalline in nature. The shape of a biofloculant also influences the flocculation efficiency of the biofloculant by forming large flocs when they make contact with other molecules or pollutants in wastewater, which makes it easy to separate the precipitation from supernatant in a solution [52]. The shape of CuNPs appeared to be cloud-like with soft edges, which may imply that the CuNPs are agglomerated. The image of SEM analysis showed a spherical-shaped biofloculant produced from *Alcaligenes faecalis* HCB2 [49]. The shape of the CuNPs is beneficial to the agglomeration of the particles to waste particles and the formation of flocs during application in wastewater treatment. In the study by Sagadevan and Koteeswari [53], the biosynthesized CuNPs were studied using SEM analysis, and they appeared to be cloud-like in shape.

### 3.3.5. TEM analysis of the biofloculant and CuNPs.

The transmission electron microscope was utilized to establish the crystal structure and morphology of the biofloculant and CuNPs. The TEM images are displayed in Figure 5.

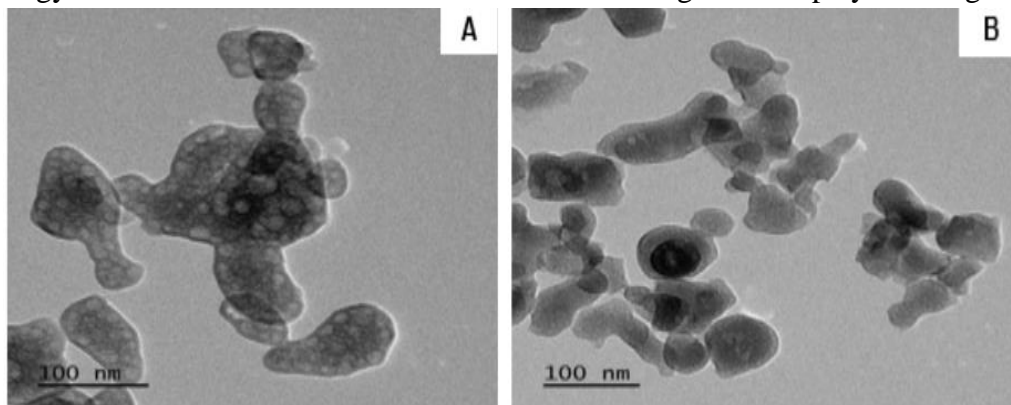


**Figure 5.** TEM images of the (a) biofloculant; (b) As-synthesized CuNPs at 100 nm.

The TEM images of the biofloculant appeared to have an amorphous outer carbon shell and spherical shape inside. The biofloculant particles are agglomerated and clustered together (Figure 5a). The morphology of the biofloculant is uniform, indicating that the biofloculant is crystalline [54]. The CuNPs appeared to be spherical (Figure 5b). The average

particle size of CuNPs was found to be approximately 35 nm. The particle size was calculated using Debye-Scherrer's equation, and the particle size was found to be approximately 33 nm. Therefore, the particle size of the particles ranges between 30 – 35 nm. Otherwise, copper nanoparticles would have agglomerated and produced a larger nanoparticle. Comparable results were reported in the study by Murthy et al. [55], where copper nanoparticles synthesized from *Hagenia abyssinica* leaf extract were reported with an average size of 34.76 nm. The average size of the CuNPs biosynthesized from *Cissus arnotiana* plant extract was within the range of 60-90 nm [56].

### 3.3.6. TGA analysis of the bioflocculant and CuNPs.

TGA analysis was applied to regulate the thermal stability of the bioflocculant and copper nanoparticles at elevated temperatures. TGA helps with understanding the pyrolysis of CuNPs and the bioflocculant [57]. The temperature from 30 to 900°C was used in determining the copper nanoparticles and the bioflocculant thermogravimetric ability, and the results are displayed in Figure 6.

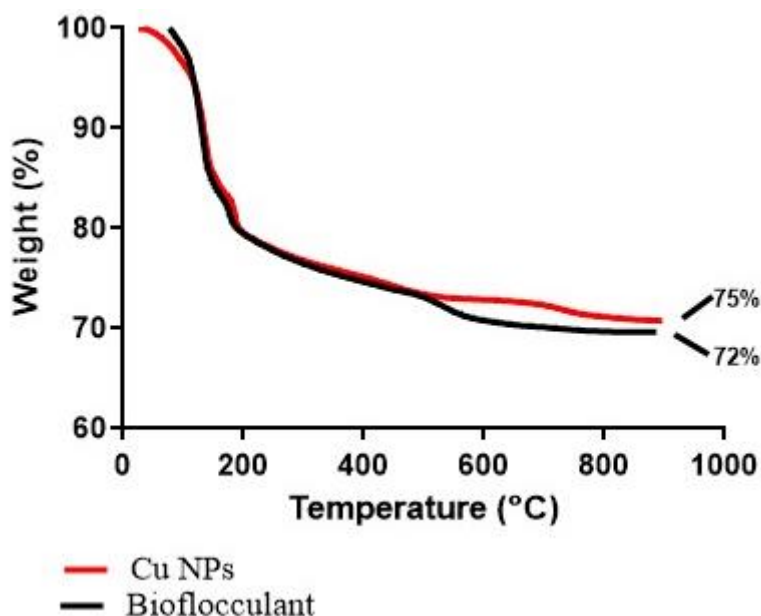


**Figure 6.** TGA for the bioflocculant and biosynthesized copper nanoparticles.

The thermogravimetric study of a bioflocculant shows that as the temperature increased, the weight loss decreased (Figure 6). At temperatures of 80 and 200°C, about 20% of the initial weight loss was observed. The primary weight loss of about 20% was detected between 80 and 200°C. This decrease in weight was ascribed to moisture content loss during elevated temperatures. The presence of moisture content is attributed to the presence of carboxyl and hydroxyl groups in the bioflocculant [58]. At the temperature between 150-190°C, a weight loss of 4% was observed, which indicated the degradation of the bioflocculant components. Another degradation was observed between 500 - 900°C with a weight loss of approximately 2%. In the temperature between 200 to 400°C, a decrease in weight was observed to be 4%, and 5% weight loss was observed in the temperature between 500 to 900°C. Further weight loss of the bioflocculant was observed due to an increase in temperature from 200°C to 900°C. Nkosi et al. [59] reported a weight loss of about 23% between 40 and 400°C using a bioflocculant extracted from *Proteus mirabilis* AB. 932526.1. TGA showed that the bioflocculant produced by *M. paraoxydans* is thermostable with a total of 72% weight retained after exposure to 90°C.

Thermogravimetric analysis of copper nanoparticles revealed a decrease in weight loss of about 20% from 30 to 180°C due to the decrease in moisture content. The degradation of CuNPs components was observed at a temperature between 115-187°C because of the increase in temperature, which leads to a deterioration of CuNPs, resulting in the loss of the material components. Another degradation pattern was observed between 530 - 730°C, which is the result of an extreme increase in temperature. About 10% weight loss was observed from 200 to 900°C. This is due to a further decrease in moisture by the material. Copper nanoparticles retained about 75% of their weight after exposure to 900 °C, confirming their thermal stability. In the study by Dlamini et al. [60], the weight of the bimetallic iron and copper nanoparticle samples at 800°C was above 50%, signifying that the materials are thermostable.

### 3.3.7. XRD analysis of the bioflocculant and CuNPs.

The XRD analysis of the bioflocculant and CuNPs was performed to reveal the crystallinity of the bioflocculant and CuNPs by measuring the intensity over dispersal angles of the X-ray [28]. Strong peaks were observed at the spectrum from 10 to 45°, which indicated the crystallinity of the bioflocculant. The peaks were observed to be weak from 45 to 80°, which contributes to the shape of the bioflocculant. Strong diffraction peaks of the bioflocculant were also reported between 10 to 40° [61]. Figure 7 shows the metallic nature of copper nanoparticles.

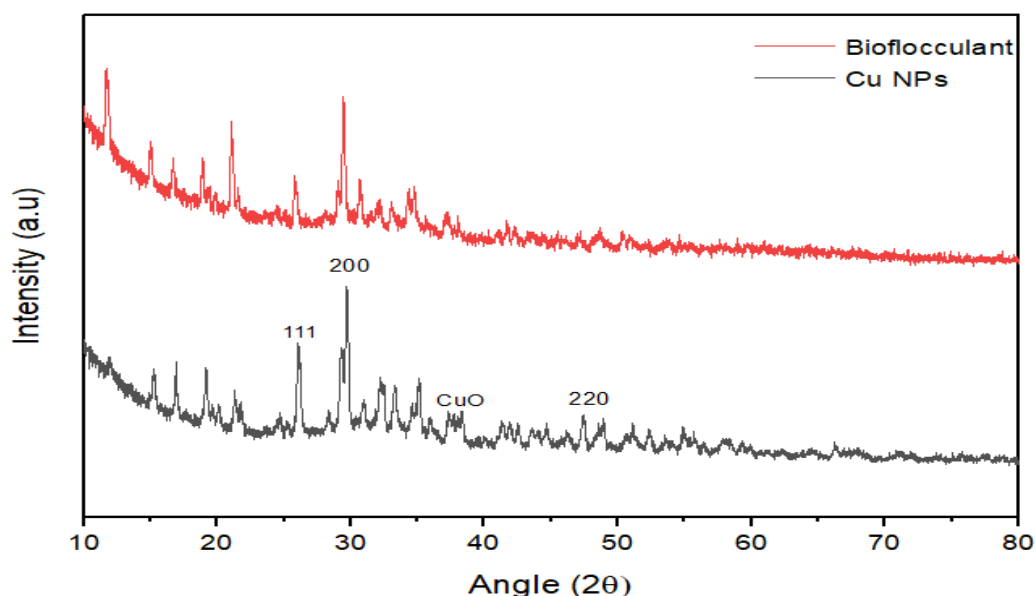


**Figure 7.** X-ray diffraction of the bioflocculant and biosynthesized CuNPs.

XRD pattern's angles ( $2\theta$ ) range from 10° to 80°. The strong peaks were observed at 11.67°, 21°, 25.67°, 29.33°, and 34.33°, which show that the synthesized copper nanoparticles are crystalline in nature. The CuNPs were synthesized successfully, as revealed by the spectrum. These values communicate with the diffraction data that shows that CuNPs have face-centered cubic structure (FCC) with diffraction peaks of (111), (200), and (220) [62, 63]. In another study, copper nanoparticles were analyzed using XRD analysis, and the results demonstrated three sharp peaks at 43.6°, 50.80°, and 74.4° angles [64]. The peak positions of CuNPs agreed with JCPDS card No: 05-0667. The average particle size was found to be 33 nm using Debye-Scherrer's equation. Meanwhile, 30 nm was found in the study by Khanna et al. [65].

## 4. Conclusions

The bioflocculant extracted from *Microbacterium paraoxydans* was successfully utilized in the production of CuNPs as a capping and reducing agent. UV-Vis analysis, FT-IR, TEM, SEM, TGA, and XRD were used to determine the characteristic properties of the synthesized CuNPs. Various functional groups reported in CuNPs included hydroxyl (O-H), amine (N-H), (C-H), and Cu-O for CuNPs, which are found to be responsible for the enhancement of flocculation efficiency. The XRD shows that the CuNPs and the bioflocculant were crystalline in nature. The approximately 33 nm particle size of CuNPs was determined using Debye's equation. The EDX analysis of CuNPs showed C (34.28 wt %), O (30.23 wt %), and Cu (20.69 wt %), confirming the biosynthesis of CuNPs using a bioflocculant with carbon (12.15 wt %) and oxygen (50.93 wt %). These elements are known to have an impact on their flocculation ability. The SEM image of the bioflocculant appeared to be rod-shaped, and the CuNPs were cloud-like in shape. TEM analysis showed an irregular spherical shape of CuNPs with an average grain size of 35 nm for CuNPs, which corresponds to the one calculated using the XRD pattern. The UV-Vis analysis of CuNPs showed absorption peaks at 549 nm, respectively, which confirmed the successful biosynthesis of CuNPs using bioflocculant. TGA analysis of CuNPs showed a weight loss of 25% for CuNPs, compared to a 28% weight loss of the bioflocculant used for their preservation, indicating that CuNPs are thermostable.

## Author Contributions

Conceptualization, A.K.B. and R.V.S.R.P., and Z.G.N.; methodology, N.P.M.; validation, A.K.B., R.V.S.R.P and Z.G.N.; formal analysis, N.P.M. and R.V.S.R.P; investigation, N.P.M.; writing-original draft preparation.; N.P.M.; writing –review and editing, Z.G.N. and R.V.S.R.P.; visualization, N.P.M.; supervision, A.K.B. and R.V.S.R.P.; project administration, Z.G.N. All authors read and agreed to the published version of the manuscript.

## Institutional Review Board Statement

Not applicable.

## Informed Consent Statement

Not applicable

## Data Availability Statement

The data supporting the findings of this study are available in the form of a thesis archived in the University of Zululand Library.

## Funding

Rajasekhar Pullabhotla would like to acknowledge the National Research Foundation (NRF, South America) for their financial support in the form of the Incentive Fund Grant (grant no. 103691) and the Research Developmental Grant for Rated Researchers (112145).

## Acknowledgments

Nokwanda Myeni appreciates the financial support of the National Research Foundation (NRF, South Africa) in the form of a master's bursary. The authors acknowledge the University of KwaZulu-Natal Electron Microscopy Unit, Westville campus, for allowing us to use the TEM, TGA, and SEM-EDX machines to characterize our nanoparticles.

## Conflicts of Interest

The authors declare no ethical conflict.

## References

1. Abdel-Aziz, S.M.; Hamed, H.A.; Mouafi, F.E.; Abdelwahed, N.A. Extracellular metabolites produced by a novel strain, *Bacillus alvei* NRC-14: 3. Synthesis of a bioflocculant that has chitosan-like structure. *Life Sci. J.* **2011**, *8*, 21-33, <https://doi.org/10.1016/j.eurpolymj.2017.01.008>.
2. Pillai, S.B.; Thombre, N.V. Coagulation, Flocculation, and Precipitation in Water and Used Water Purification. In *Handbook of Water and Used Water Purification*, Lahnsteiner, J., Ed.; Springer International Publishing: Cham, **2024**; pp. 1-25, [https://doi.org/10.1007/978-3-319-66382-1\\_63-1](https://doi.org/10.1007/978-3-319-66382-1_63-1)
3. Nontembiso, P.; Sekelwa, C.; Leonard, M.V.; Anthony, O.I. Assessment of bioflocculant production by *Bacillus* sp. Gilbert, a marine bacterium isolated from the bottom sediment of Algoa Bay. *Mar. Drugs.* **2011**, *9*, 1232-1242, <https://doi.org/10.3390/md9071232>.
4. Sekelwa, C.; Anthony, U.M.; Vuyani, M.L.; Anthony, O.I. Characterization of a thermostable polysaccharide bioflocculant produced by *Virgibacillus* species isolated from Algoa bay. *Afr. J. Microbiol. Res.* **2013**, *7*, 2925-2938, <https://doi.org/10.5897/AJMR12.2371>.
5. Ntsangani, N.; Okaiyeto, K.; Uchchukwu, N.U.; Olaniran, A.O.; Mabinya, L.V.; Okoh, A.I. Bioflocculation potentials of a uronic acid-containing glycoprotein produced by *Bacillus* sp. AEMREG4 isolated from Tyhume River, South Africa. *3 Biotech* **2017**, *7*, 78, <https://doi.org/10.1007%2Fs13205-017-0695-8>.
6. Kurniawan, S.B.; Ahmad, A.; Imron, M.F.; Abdullah, S.R.S.; Othman, A.R.; Hasan, H.A. Potential of microalgae cultivation using nutrient-rich wastewater and harvesting performance by biocoagulants/bioflocculants: Mechanism, multi-conversion of biomass into valuable products, and future challenges. *J. Clean. Prod.* **2022**, *365*, 132806, <https://doi.org/10.1016/j.jclepro.2022.132806>.
7. Ugbenyen, A.; Cosa, S.; Mabinya, L.; Babalola, O.O.; Aghdasi, F.; Okoh, A. Thermostable bacterial bioflocculant produced by *Cobetia* spp. isolated from Algoa Bay (South Africa). *Int. J. Environ. Res. Public Health.* **2012**, *9*, 2108-2120, <https://doi.org/10.3390/ijerph9062108>.
8. Oyewole, O.A.; Jagaba, A.; Abdulhammed, A.A.; Yakubu, J.G.; Maude, A.M.; Abioye, O.P.; Adeniyi, O.D.; Egwim, E.C. Production and characterization of a bioflocculant produced by microorganisms isolated from earthen pond sludge. *Bioresour. Technol. Reports.* **2023**, *22*, 101492, <https://doi.org/10.1016/j.biteb.2023.101492>.
9. Zheng, L.; Zhou, M.; Guo, Z.; Lu, H.; Qian, L.; Dai, H.; Qiu, J.; Yakubovskaya, E.; Bogenhagen, D.F.; Demple, B. Human DNA2 is a mitochondrial nuclease/helicase for efficient processing of DNA replication and repair intermediates. *Mol. Cell.* **2008**, *32*, 325-336, <https://doi.org/10.1016/j.molcel.2008.09.024>.
10. Czemińska, M.; Szcześ, A.; Hołysz, L.; Wiater, A.; Jarosz-Wilkolazka, A. Characterisation of exopolymer R-202 isolated from *Rhodococcus rhodochrous* and its flocculating properties. *European Polymer Journal.* **2017**, *88*, 21-33, <https://doi.org/10.1016/j.eurpolymj.2017.01.008>.
11. He, J.; Zou, J.; Shao, Z.; Zhang, J.; Liu, Z.; Yu, Z. Characteristics and flocculating mechanism of a novel bioflocculant HBF-3 produced by deep-sea bacterium mutant *Halomonas* sp. V3a'. *Worl. J. Microbiol. Biotechnol.* **2010**, *26*, 1135-1141, <http://dx.doi.org/10.1007%2Fs11274-009-0281-2>.
12. Ahire, S.A.; Bachhav, A.A.; Pawar, T.B.; Jagdale, B.S.; Patil, A.V.; Koli, P.B. The Augmentation of nanotechnology era: A concise review on fundamental concepts of nanotechnology and applications in material science and technology. *Results Chem.* **2022**, *4*, 100633, <https://doi.org/10.1016/j.rechem.2022.100633>.

13. Tamilvanan, A.; Balamurugan, K.; Ponappa, K.; Kumar, B.M. Copper nanoparticles: synthetic strategies, properties and multifunctional application. *Int. J. Nanosci.* **2014**, *13*, 1430001, <https://doi.org/10.1142/S0219581X14300016>.
14. Zabed, H.M.; Islam, J.; Chowdhury, F.I.; Zhao, M.; Awasthi, M.K.; Nizami, A.-S.; Uddin, J.; Thomas, S.; Qi, X. Recent insights into heterometal-doped copper oxide nanostructure-based catalysts for renewable energy conversion and generation. *Renew. Sustain. Energy Rev.* **2022**, *168*, 112887, <https://doi.org/10.1016/j.rser.2022.112887>.
15. Sierra-Ávila, R.; Pérez-Alvarez, M.; Cadenas-Pliego, G.; Comparán Padilla, V.; Ávila-Orta, C.; Pérez Camacho, O.; Jiménez-Regalado, E.; Hernández-Hernández, E.; Jiménez-Barrera, R.M. Synthesis of copper nanoparticles using mixture of allylamine and polyallylamine. *J. Nanomater.* **2015**, *2015*, 367341, <https://doi.org/10.1155/2015/367341>.
16. Betancourt-Galindo, R.; Reyes-Rodriguez, P.; Puente-Urbina, B.; Avila-Orta, C.; Rodríguez-Fernández, O.; Cadenas-Pliego, G.; Lira-Saldivar, R.; García-Cerda, L. Synthesis of copper nanoparticles by thermal decomposition and their antimicrobial properties. *J. Nanomat.* **2014**, *2014*, 980545, <https://doi.org/10.1155/2014/980545>.
17. Salavati-Niasari, M.; Davar, F. Synthesis of copper and copper (I) oxide nanoparticles by thermal decomposition of a new precursor. *Mater. Lett.* **2009**, *63*, 441-443, <https://doi.org/10.1016/j.matlet.2008.11.023>.
18. Ijaz, I.; Gilani, E.; Nazir, A.; Bukhari, A. Detail review on chemical, physical and green synthesis, classification, characterizations and applications of nanoparticles. *GCLR.* **2020**, *13*, 223-245, <https://doi.org/10.1080/17518253.2020.1802517>.
19. Jardón-Maximino, N.; Pérez-Alvarez, M.; Sierra-Ávila, R.; Ávila-Orta, C.A.; Jiménez-Regalado, E.; Bello, A.M.; González-Morones, P.; Cadenas-Pliego, G. Oxidation of copper nanoparticles protected with different coatings and stored under ambient conditions. *J. Nanomater.* **2018**, *2018*, 9512768, <https://doi.org/10.1155/2018/9512768>.
20. Gawande, M.B.; Goswami, A.; Felpin, F.-X.; Asefa, T.; Huang, X.; Silva, R.; Zou, X.; Zboril, R.; Varma, R.S. Cu and Cu-based nanoparticles: synthesis and applications in catalysis. *Chem. rev.* **2016**, *116*, 3722-3811, <https://doi.org/10.1021/acs.chemrev.5b00482>.
21. Maliki, M.; Ifijen, I.H.; Ikhuoria, E.U.; Jonathan, E.M.; Onaiwu, G.E.; Archibong, U.D.; Ighodaro, A. Copper nanoparticles and their oxides: optical, anticancer and antibacterial properties. *Int. Nano Lett.* **2022**, *12*, 379-398, <https://doi.org/10.1007/s40089-022-00380-2>.
22. Goldern, N.; Kotze, B.; Evelyn, M.; Rajasekhar, P.; Singh, M. Removal efficiency of a thermostable and non-toxic bioflocculant produced by a consortium of two marine bacteria. *Biosci. Res.* **2020**, *18*, 1288, <https://doi.org/10.3389/fmicb.2019.01288>.
23. Tsilo, P.H.; Basson, A.K.; Ntombela, Z.G.; Dlamini, N.G.; Pullabhotla, R.V. Biosynthesis and characterization of copper nanoparticles using a bioflocculant produced by a yeast *Pichia kudriavzevii* isolated from Kombucha tea SCOBY. *Appl. Nano.* **2023**, *4*, 226-239, <https://doi.org/10.3390/applnano4030013>.
24. Tsilo, P.H.; Basson, A.K.; Ntombela, Z.G.; Dlamini, N.G.; Pullabhotla, R.V. Green synthesis and characterisation of silver nanoparticles utilising a bioflocculant obtained from *Pichia kudriavzevii* isolated from kombucha tea SCOBY. *Adv. Mater. Proces. Technol.* **2024**, 1-17, <https://doi.org/10.1080/2374068X.2024.2379677>.
25. Lobregas, M.O.S.; Camacho, D.H. Chapter 2 - Green synthesis of copper-based nanoparticles using microbes. In *Copper Nanostructures: Next-Generation of Agrochemicals for Sustainable Agroecosystems*, Abd-Elsalam, K.A., Ed.; Elsevier: **2022**; pp. 17-44, <https://doi.org/10.1016/B978-0-12-823833-2.00012-X>.
26. Pérez-Alvarez, M.; Cadenas-Pliego, G.; Pérez-Camacho, O.; Comparán-Padilla, V.E.; Cabello-Alvarado, C.J.; Saucedo-Salazar, E. Green synthesis of copper nanoparticles using cotton. *Polymers* **2021**, *13*, 1906, <https://doi.org/10.3390/polym13121906>.
27. Pandey, B.; Pathak, J.; Singh, P.; Kumar, R.; Kumar, A.; Kaushik, S.; Thakur, T.K. Microplastics in the ecosystem: an overview on detection, removal, toxicity assessment, and control release. *Water* **2023**, *15*, 51, <https://doi.org/10.3390/w15010051>.
28. Li, X.; Robinson, S.M.; Gupta, A.; Saha, K.; Jiang, Z.; Moyano, D.F.; Sahar, A.; Riley, M.A.; Rotello, V.M. Functional gold nanoparticles as potent antimicrobial agents against multi-drug-resistant bacteria. *ACS Nano.* **2014**, *8*, 10682-10686, <https://doi.org/10.1021/nn5042625>.

29. Salgado, P.; Márquez, K.; Vidal, G. Biogenic Synthesis Based on Cuprous Oxide Nanoparticles Using Eucalyptus globulus Extracts and Its Effectiveness for Removal of Recalcitrant Compounds. *Catalysts*. **2024**, *14*, 525, <https://doi.org/10.3390/catal14080525>.
30. Ntombela, Z.; Mthembu, N.; Gasa, N.; Basson, A.; Simonis, J.; Madoroba, E.; Pullabhotla, V. Isolation, identification, and characterization of a bioflocculant producing strain, *Bacillus* sp. KC782848. 1, from umlalazi catchment, Mtunzini, KwaZulu-Natal. *Biosci. Res.* **2019**, *16*, 3664-3685.
31. Makapela, B.; Okaiyeto, K.; Ntozonke, N.; Nwodo, U.U.; Green, E.; Mabinya, L.V.; Okoh, A.I. Assessment of *Bacillus pumilus* isolated from fresh water milieu for bioflocculant production. *Appl. Sci.* **2016**, *6*, 211, <https://doi.org/10.3390/app6080211>.
32. Liu, W.; He, R.; Liu, C. An alkali-tolerant strain *Microbacterium esteraromaticum* C26 produces a high yield of cation-independent bioflocculant. *AIMS Environ. Sci.* **2016**, *3*, 408-419, <https://doi.org/10.3934/environsci.2016.3.408>.
33. Ismail, M.; Gul, S.; Khan, M.; Khan, M.A.; Asiri, A.M.; Khan, S.B. Green synthesis of zerovalent copper nanoparticles for efficient reduction of toxic azo dyes congo red and methyl orange. *GPS* **2019**, *8*, 135-143, <https://doi.org/10.1515/gps-2018-0038>.
34. Dlamini, N.G.; Basson, A.K.; Pullabhotla, V.S.R. Optimization and application of bioflocculant passivated copper nanoparticles in the wastewater treatment. *Int. J. Environ. Res. Public Health.* **2019**, *16*, 2185, <https://doi.org/10.3390/ijerph16122185>.
35. Yang, Q.; Zhao, X.; Zhang, J.; Wang, Y.; Zou, W.; Ming, H.; Zhao, C. Components of a Bioflocculant for Treating Tannery Wastewater. *Journal of Residuals Science & Technology* **2015**, *12*, 99-103.
36. Bakhsh, E.M.; Ali, F.; Khan, S.B.; Marwani, H.M.; Danish, E.Y.; Asiri, A.M. Copper nanoparticles embedded chitosan for efficient detection and reduction of nitroaniline. *Int. J. Biol. Macromol.* **2019**, *131*, 666-675, <https://doi.org/10.1016/j.ijbiomac.2019.03.095>.
37. Amer, M.; Awwad, A. Green synthesis of copper nanoparticles by *Citrus limon* fruits extract, characterization and antibacterial activity. *Chem. Int.* **2021**, *7*, 1-8, <https://doi.org/10.5281/zenodo.4017993>.
38. Lv, Q.; Zhang, B.; Xing, X.; Zhao, Y.; Cai, R.; Wang, W.; Gu, Q. Biosynthesis of copper nanoparticles using *Shewanella loihica* PV-4 with antibacterial activity: novel approach and mechanisms investigation. *J. Hazard. Mater.* **2018**, *347*, 141-149, <https://doi.org/10.1016/j.jhazmat.2017.12.070>.
39. Sriramulu, M.; Shanmugam, S.; Ponnusamy, V.K. *Agaricus bisporus* mediated biosynthesis of copper nanoparticles and its biological effects: An in-vitro study. *J. Colloid Interface Sci.* **2020**, *35*, 100254, <https://doi.org/10.1016/j.colcom.2020.100254>.
40. Rajesh, K.; Ajitha, B.; Reddy, Y.A.K.; Suneetha, Y.; Reddy, P.S. Assisted green synthesis of copper nanoparticles using *Syzygium aromaticum* bud extract: Physical, optical and antimicrobial properties. *Optik* **2018**, *154*, 593-600, <https://doi.org/10.1016/j.ijleo.2017.10.074>.
41. Ntozonke, N.; Okaiyeto, K.; Okoli, A.S.; Olaniran, A.O.; Nwodo, U.U.; Okoh, A.I. A marine bacterium, *Bacillus* sp. isolated from the sediment samples of Algoa Bay in South Africa Produces a Polysaccharide-Bioflocculant. *Int. J. Environ. Res. Public Health* **2017**, *14*, 1149, <https://doi.org/10.3390/ijerph14101149>.
42. Pathak, M.; Devi, A.; Bhattacharyya, K.; Sarma, H.; Subudhi, S.; Lal, B. Production of a non-cytotoxic bioflocculant by a bacterium utilizing a petroleum hydrocarbon source and its application in heavy metal removal. *RSC Adv.* **2015**, *5*, 66037-66046, <https://doi.org/10.1039/C5RA08636A>.
43. Kurniawan, S.B.; Imron, M.F.; Chik, C.E.N.C.E.; Owodunni, A.A.; Ahmad, A.; Alnawajha, M.M.; Rahim, N.F.M.; Said, N.S.M.; Abdullah, S.R.S.; Kasan, N.A. What compound inside biocoagulants/bioflocculants is contributing the most to the coagulation and flocculation processes? *Sci Total Env.* **2022**, *806*, 150902, <https://doi.org/10.1016/j.scitotenv.2021.150902>.
44. Okaiyeto, K.; Nwodo, U.U.; Mabinya, L.V.; Okoh, A.I. Characterization of a bioflocculant produced by a consortium of *Halomonas* sp. Okoh and *Micrococcus* sp. Leo. *Int. J. Environ. Res. Public Health* **2013**, *10*, 5097-5110, <https://doi.org/10.3390/ijerph10105097>.
45. Xiong, Y.; Wang, Y.; Yu, Y.; Li, Q.; Wang, H.; Chen, R.; He, N. Production and characterization of a novel bioflocculant from *Bacillus licheniformis*. *Appl. Environ. Microbiol.* **2010**, *76*, 2778-2782, <https://doi.org/10.1128/AEM.02558-09>.
46. Ntombela, Z.; Kubhayi, T.; Basson, A.; Simonis, J.; Madoroba, E.; Pullabhotla, V. Characterization of bioflocculant produced by *Bacillus* species isolated from uMlalazi estuary, Mthunzini area (KwaZulu-Natal) and its application in wastewater treatment. *Biosci. Res.* **2020**, *17*, 1944-1970.

47. Mohamed, E.A. Green synthesis of copper & copper oxide nanoparticles using the extract of seedless dates. *Heliyon* **2020**, *6*, e03123, <https://doi.org/10.1016/j.heliyon.2019.e03123>.
48. Aher, H.; Han, S.; Vikhe, A.; Kuchekar, S. Green synthesis of copper nanoparticles using *Syzygium Cumini* leaf extract, characterization and antimicrobial activity. *Chem. Sci. Trans.* **2019**, *8*, 1-6.
49. Maliehe, T.S.; Basson, A.K.; Dlamini, N.G. Removal of pollutants in mine wastewater by a non-cytotoxic polymeric bioflocculant from *Alcaligenes faecalis* HCB2. *Int. J. Environ. Res. Public Health.* **2019**, *16*, 4001, <https://doi.org/10.3390/ijerph16204001>.
50. Agunbiade, M.; Pohl, C.; Ashafa, O. Bioflocculant production from *Streptomyces platensis* and its potential for river and waste water treatment. *Braz. J. Microbiol.* **2018**, *49*, 731-741, <https://doi.org/10.1016/j.bjm.2017.02.013>.
51. El-Saadony, M.T.; Abd El-Hack, M.E.; Taha, A.E.; Fouda, M.M.; Ajarem, J.S.; N. Maodaa, S.; Allam, A.A.; Elshaer, N. Ecofriendly synthesis and insecticidal application of copper nanoparticles against the storage pest *Tribolium castaneum*. *Nanomaterials* **2020**, *10*, 587, <https://doi.org/10.3390/nano10030587>.
52. Abu Tawila, Z.M.; Ismail, S.; Dadrasnia, A.; Usman, M.M. Production and characterization of a bioflocculant produced by *Bacillus salmalaya* 139SI-7 and its applications in wastewater treatment. *Mol.* **2018**, *23*, 2689, <https://doi.org/10.3390/molecules23102689>.
53. Sagadevan, S.; Koteeswari, P. Analysis of structure, surface morphology, optical and electrical properties of copper nanoparticles. *Nanomed. J. Res.* **2015**, *2*, 00040-00048, <https://doi.org/10.15406/jnmr.2015.02.00040>.
54. Habibi, M.H.; Kamrani, R.; Mokhtari, R. Fabrication and characterization of copper nanoparticles using thermal reduction: the effect of nonionic surfactants on size and yield of nanoparticles. *Microchimic. Acta* **2010**, *171*, 91-95, <https://doi.org/10.1007/s00604-010-0413-2>.
55. Murthy, H.A.; Desalegn, T.; Kassa, M.; Abebe, B.; Assefa, T. Synthesis of green copper nanoparticles using medicinal plant *Hagenia abyssinica* (Brace) JF. Gmel. leaf extract: Antimicrobial properties. *J. Nanomater.* **2020**, *2020*, 3924081, <https://doi.org/10.1155/2020/3924081>.
56. Rajeshkumar, S.; Menon, S.; Kumar, S.V.; Tambuwala, M.M.; Bakshi, H.A.; Mehta, M.; Satija, S.; Gupta, G.; Chellappan, D.K.; Thangavelu, L. Antibacterial and antioxidant potential of biosynthesized copper nanoparticles mediated through *Cissus arnotiana* plant extract. *J. Photochem. Photobiol. B* **2019**, *197*, 111531, <https://doi.org/10.1016/j.jphotobiol.2019.111531>.
57. Vimala, R.; Escaline, J.L.; Sivaramakrishnan, S. Characterization of self-assembled bioflocculant from the microbial consortium and its applications. *JEM* **2020**, *258*, 110000, <https://doi.org/10.1016/j.jenvman.2019.110000>.
58. Wang, L.; Ma, F.; Qu, Y.; Sun, D.; Li, A.; Guo, J.; Yu, B. Characterization of a compound bioflocculant produced by mixed culture of *Rhizobium radiobacter* F2 and *Bacillus sphaeicus* F6. *JMB* **2011**, *27*, 2559-2565, <https://doi.org/10.1007/s11274-011-0726-2>.
59. Nkosi, N.C.; Basson, A.K.; Ntombela, Z.G.; Maliehe, T.S.; Pullabhotla, R.V. Isolation, identification and characterization of bioflocculant-producing bacteria from activated sludge of Vulindlela Wastewater Treatment Plant. *Appl. Microbiol.* **2021**, *1*, 586-606, <https://doi.org/10.3390/applmicrobiol1030038>.
60. Dlamini, N.G.; Basson, A.K.; Pullabhotla, V.S.R. A Comparative study between Bimetallic Iron@ copper nanoparticles with iron and copper nanoparticles synthesized Using a bioflocculant: Their applications and biosafety. *Processes* **2020**, *8*, 1125, <https://doi.org/10.3390/pr8091125>.
61. Tsilo, P.H.; Basson, A.K.; Ntombela, Z.G.; Maliehe, T.S.; Pullabhotla, R.V. Isolation and optimization of culture conditions of a bioflocculant-producing fungi from Kombucha tea SCOBY. *Microbiol. Res.* **2021**, *12*, 950-966, <https://doi.org/10.3390/microbiolres12040070>.
62. Khalid, H.; Shamaila, S.; Zafar, N.. Synthesis of copper nanoparticles by chemical reduction method. *Sci. Int.* **2015**, *27*, 3085-3088, <https://doi.org/10.1007/s00253-018-9145-8>.
63. Musa, A.; Mohammed, A.H.; Ahmad, M.; Musah, M. Copper Nanoparticles Synthesized in Biopolymer Matrix and Their Application in Antibacterial Activity. *Baghdad Sci. J.* **2024**, *21*, 1055-1055, <https://dx.doi.org/10.21123/bsj.2023.8831>.
64. Ahmadi-Nouraldinwand, F.; Afrouz, M.; Elias, S.G.; Eslamian, S. Green synthesis of copper nanoparticles extracted from guar seedling under Cu heavy-metal stress by *Trichoderma harzianum* and their bio-efficacy evaluation against *Staphylococcus aureus* and *Escherichia coli*. *Environ. Earth Sci.* **2022**, *81*, 54, <https://doi.org/10.1007/s12665-022-10184-4>.
65. Khanna, P.; Gaikwad, S.; Adhyapak, P.; Singh, N.; Marimuthu, R. Synthesis and characterization of copper nanoparticles. *Mater. Lett.* **2007**, *61*, 4711-4714, <https://doi.org/10.1016/j.matlet.2007.03.014>.

## **Publisher's Note & Disclaimer**

The statements, opinions, and data presented in this publication are solely those of the individual author(s) and contributor(s) and do not necessarily reflect the views of the publisher and/or the editor(s). The publisher and/or the editor(s) disclaim any responsibility for the accuracy, completeness, or reliability of the content. Neither the publisher nor the editor(s) assume any legal liability for any errors, omissions, or consequences arising from the use of the information presented in this publication. Furthermore, the publisher and/or the editor(s) disclaim any liability for any injury, damage, or loss to persons or property that may result from the use of any ideas, methods, instructions, or products mentioned in the content. Readers are encouraged to independently verify any information before relying on it, and the publisher assumes no responsibility for any consequences arising from the use of materials contained in this publication.